

Monte Carlo study of the critical temperature for the planar rotator model with nonmagnetic impurities

S. A. Leonel and Pablo Zimmermann Coura

Departamento de Física ICE, Universidade Federal de Juiz de Fora, Juiz de Fora, CEP 36036-330, Minas Gerais, Brazil

A. R. Pereira and L. A. S. Mól

Departamento de Física, Universidade Federal de Viçosa, 36571-000, Viçosa, Minas Gerais, Brazil

B. V. Costa

Departamento de Física, ITEX, Universidade Federal de Minas Gerais, Caixa Postal 702, CEP 30123-970, Belo Horizonte, MG, Brazil

(Received 8 October 2002; published 26 March 2003)

We performed Monte Carlo simulations to calculate the Berezinskii-Kosterlitz-Thouless (BKT) temperature T_{BKT} for the two-dimensional planar rotator model in the presence of nonmagnetic impurity concentration (ρ). As expected, our calculation shows that the BKT temperature decreases as the spin vacancies increase. There is a critical dilution $\rho_c \approx 0.3$ at which $T_{BKT} = 0$. The effective interaction between a vortex-antivortex pair and a static nonmagnetic impurity is studied analytically. A simple phenomenological argument based on the pair-impurity interaction is proposed to justify the simulations.

DOI: 10.1103/PhysRevB.67.104426

PACS number(s): 75.30.Hx, 75.40.Mg, 75.10.Hk, 74.78.-w

I. INTRODUCTION

The planar rotator (PR) model in two dimensions (2D) is a prototype for several physical systems such as, for example, high-temperature superconductors and granular superconductors. The PR model supports topological excitations, and although there is no long-range order at any finite temperature, it undergoes a Berezinskii-Kosterlitz-Thouless (BKT) phase transition driven by the unbinding of vortex-antivortex pairs. In short the BKT picture of the phase transition is as follows. At low temperature spin waves are the relevant excitations of the system. Spin-spin correlation functions fall off slowly with distance; free vortices do not exist but pairs strongly bind. Vortices pairs cannot disorder the system significantly since they affect only close spins. As the temperature is raised, the distance between vortex-antivortex pairs grows until T_{BKT} . Then free vortices exist, the system is disordered, and the spin-spin correlation function falls off exponentially. The Hamiltonian describing the model is

$$H = - \sum_{\langle i,j \rangle} J_{i,j} \vec{S}_i \cdot \vec{S}_j, \quad (1)$$

where i and j enumerate sites in a square lattice, $J_{i,j}$ is an exchange coupling, and $\vec{S}_i = \{S_i^x, S_i^y\} = |S| \{\cos \theta_i, \sin \theta_i\}$ is a two-dimensional spin vector. Of course, Hamiltonian (1) describes an ideal system, in which each site of a regular square lattice is occupied by a spin vector \vec{S} . However, impurities and/or defects are present in any material sample. In fact, the effect of impurities on superconductors has been of theoretical and experimental interest in its own right for a long time. Particularly, the interaction of topological excitations with spatial inhomogeneities is of considerable importance from both theoretical and applied points of view. For example,

solitons near a nonmagnetic impurity in 2D antiferromagnets cause observable effects in electron paramagnetic resonance (EPR) experiments.^{1,2} In this scenario it would be important to study the effects of the presence of nonmagnetic sites diluted in magnetic materials. In a recent work, Mól, Pereira, and Pires³ have studied the interaction between a static spin vacancy and a planar vortex, and they have shown that the effective potential experienced between the two defects is repulsive. It indicates that the presence of spinless atoms on the magnetic plane may affect the BKT critical temperature. The main goal in this paper is to consider the effect of magnetic dilution to the BKT temperature by using numerical and analytical methods. To take into account the presence of nonmagnetic impurities in our model [Eq. (1)] we can replace some spin vector \vec{S} by a $\vec{S} = 0$ creating a vacancy at that lattice site. First we consider that the spin vacancies are uniformly distributed on the sites of the lattice. The case in which the spin vacancies are grouped into a cluster will also be analyzed in order to compare with the random case.

The paper is organized as follows: in Sec. II, we describe the model and the Monte Carlo (MC) method. In Sec. III we present the MC results. In Sec. IV, the continuum theory is used to study the vortex-pair-impurity interaction and a simple heuristic argument to justify the MC results is presented, and Sec. V contains a summary and final comments.

II. BACKGROUND

We consider in this work a quenched site-diluted PR model. In order to introduce dilution we define a variable σ_i with the following properties: It is 1 if site i is magnetic and 0 otherwise. To accommodate this change we have to modify Eq. (1) as

$$H = -J \sum_{\langle i,j \rangle} \sigma_i \vec{S}_i \cdot \sigma_j \vec{S}_j = -J \sum_{\langle i,j \rangle} \sigma_i \sigma_j \cos(\theta_i - \theta_j). \quad (2)$$

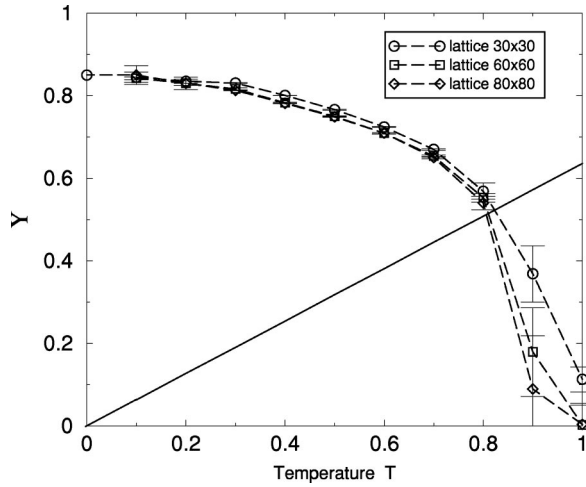


FIG. 1. Helicity modulus Y as a function of temperature for lattices with sizes 30×30 , 60×60 , and 80×80 and with 5% of nonmagnetic impurities randomly distributed. The solid line is the curve $(2/\pi)T$ and the dashed lines are only guides to the eyes.

The precise determination of the BKT temperature is a difficult task due to the absence of sharp peaks in the thermodynamic quantities. One way to extract T_{BKT} was suggested by Weber and Minnhagen^{4,5} by calculating the helicity modulus defined as

$$Y = \frac{\partial^2 F}{\partial \Delta^2}, \quad (3)$$

where F is the free energy and Δ is a small twist across the system in one direction. Using Eq. (2) we get

$$Y = -\frac{1}{2(N-n)} \langle H \rangle - \frac{1}{k_b T (N-n)} \left\langle \left[\sum_{i,j} \sigma_i \sigma_j \sin(\theta_i - \theta_j) \hat{e}_{i,j} \cdot \hat{x} \right]^2 \right\rangle, \quad (4)$$

where N is the volume of the system, n is the number of nonmagnetic sites, $\hat{e}_{i,j}$ is the vector pointing from site j to site i , and \hat{x} is a unit vector pointing along the x direction. The Kosterlitz renormalization-group equations⁶ lead to the prediction that Y jumps from the value $(2/\pi)T_c$ to zero at the critical temperature,

$$\lim_{T \rightarrow T_c} \frac{Y}{k_b T} = \frac{2}{\pi}. \quad (5)$$

Although Eq. (3) was obtained for the nondiluted mode, its extension to diluted cases is expected to be straightforward. Arguments based on the self-consistent harmonic approximation show that the helicity modulus at T_{BKT} should be independent of the nonmagnetic impurity concentration.⁷ To calculate the quantity Y we use a MC approach using a standard Metropolis algorithm with periodic boundary conditions.⁸ We used $100 \times L \times L$ Monte Carlo steps per site for equilibration, which means, for example, we moved each

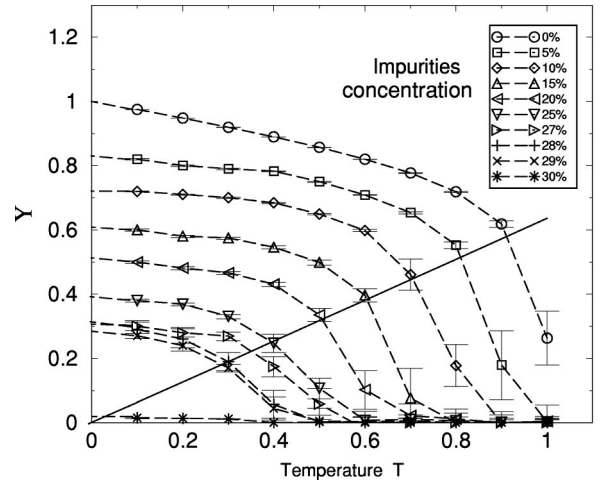


FIG. 2. Helicity modulus Y as a function of temperature for lattices size 60×60 with 0%, 5%, 10%, 15%, 20%, 25%, 27%, 28%, 29%, and 30% of nonmagnetic impurities randomly distributed. The solid line is the line $(2/\pi)T$ and dashed curves are guides to the eye.

spin 3.6×10^4 times for the $L=60$ lattice. The temperature was varied in steps of size $\Delta T=0.1$ K. Each point in our simulations is the result of the average over 2×10^5 independent configurations. In the figures showing the results of our simulations, when not indicated, the error bars are smaller than the symbols.

Figure 1 shows the results from MC simulations of Y for lattices with 5% of impurities and sizes $L=30$, 60, and 80. The straight line represents $(2/\pi)T$. The crossing point between this line and Y gives an estimate of the BKT temperature. Of course, this estimate becomes more accurate as the lattice size increases. However, as we can see in Fig. 1, the lattice of size $L=60$ already gives a good result adequate for our purposes. From now on we use $k_b=1$. The symbol T_{BKT} is used for $T_c(\rho=0)$, i.e., $T_{BKT}=T_c(\rho=0)$.

III. MONTE CARLO RESULTS

In this section we present the results obtained by MC simulations. First, we distribute the nonmagnetic impurities at random in the lattice sites. Figure 2 contains the helicity modulus as a function of the temperature considering several values of the impurity concentration (ρ). The straight line representing the function $(2/\pi)T$ is also shown. As noted earlier, the intersection of this line with the value of each Y gives T_c for the corresponding impurity concentration. We observe that $T_c(\rho)$ decreases with increasing ρ . Since the helicity modulus is a measurement of the phase correlations of the system,⁵ it is not surprising that these correlations are strongly affected by the dilution. It can be understood as follows: if we remove a spin from the lattice, the nearest neighbors of that spin will have coordination number of 3, one less than in the bulk. The spins in the boundary have larger fluctuations than the spins in the bulk lowering the spin correlations. We should expect that the fluctuation becomes appreciable, disordering the system for large enough

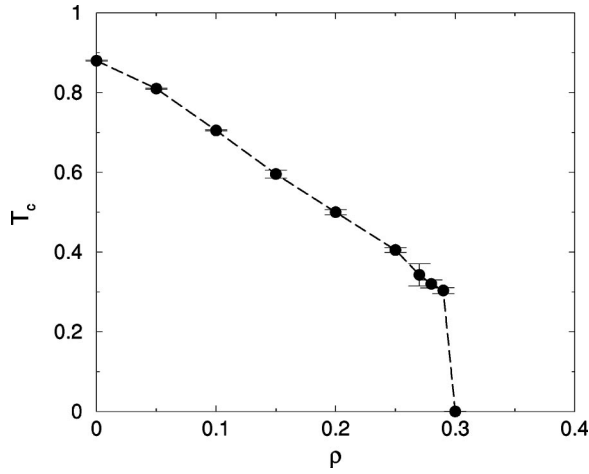


FIG. 3. The BKT transition temperature behavior as a function of nonmagnetic impurity concentration, based on the MC simulations results shown in Fig. 2. The dashed curves are guides to the eye.

nonmagnetic concentrations up to a critical value where the BKT temperature goes down to zero. In Fig. 3 we show the BKT temperature as a function of the nonmagnetic impurity concentration. Each point in our plot is the result of an average over four different distributions of nonmagnetic sites for the same concentration ρ . Note the abrupt fall of the critical temperature for $\rho_c \approx 0.3$. We also performed MC simulations for the case in which the nonmagnetic impurities are clustered for $\rho = 0.2$ and 0.3 (see Fig. 4). Note that in this case the critical temperature practically does not depend on the impurity concentration [$T_c(0.2) \approx T_c(0.3)$]. In fact this is an expected result. Since the nonmagnetic cluster is confined to a region of size $\rho \times L^2$ and the boundary grows as $\rho \times L$, spins are still strongly correlated, driving the BKT transition even for large values of ρ . A comparison between the two cases is shown in Fig. 4. Note the considerable difference between them. Due to the short range of the spin interactions, only the spins near the boundary of the cluster will become influenced by the vacancies and hence the correlations of the rest of the system will have a behavior almost independent of the vacancies. It must not affect considerably the vortices that are formed far way from the cluster and the phase transition occurs normally.

IV. VORTEX-ANTIVORTEX-IMPURITY INTERACTION

In this section we discuss the effect of nonmagnetic sites on the vortex-antivortex structure. The interaction between the topological excitation and a single nonmagnetic impurity below the critical temperature may help us to understand in more detail the phase transition mechanism. In the continuum limit, Hamiltonian (1) can be written as

$$H_c = (1/2)J \int (\vec{\nabla} \theta)^2 d^2x. \quad (6)$$

Following Ref. 3, to take into account the absence of one spin in the lattice site we modify H_c as

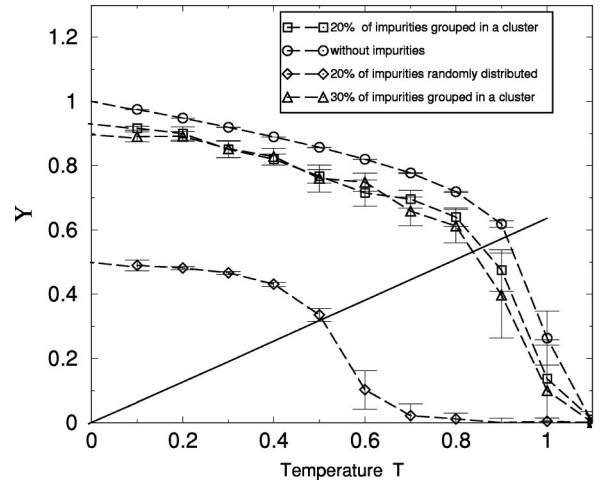


FIG. 4. Helicity modulus Y as a function of temperature, for lattices with 20% and 30% of nonmagnetic impurities grouped in a cluster, compared with the helicity modulus results for lattice with 20% of nonmagnetic impurities randomly distributed and lattice without impurities. The solid line is the line $(2/\pi)T$ and dashed curves are guides to the eye.

$$H_l = (1/2)J \int (\vec{\nabla} \theta)^2 V(\vec{r}) d^2x, \quad (7)$$

where $V(\vec{r})$ is a localized potential given by $V(\vec{r}) = 1$ if $|\vec{r} - \vec{r}_0| \geq a$ and $V(\vec{r}) = 0$ if $|\vec{r} - \vec{r}_0| < a$. Here, the nonmagnetic site is placed at \vec{r}_0 and a stands for the lattice constant. This lack of magnetic interaction inside the circle of radius a means that a spin located at \vec{r}_0 was removed from the lattice. The equation of motion obtained from Eq. (7) is

$$V(\vec{r}) \nabla^2 \theta = -\vec{\nabla} V(\vec{r}) \cdot \vec{\nabla} \theta. \quad (8)$$

In polar coordinates, the vectors \vec{r} and \vec{r}_0 are written as (r, ϕ) and (r_0, ϕ_0) , respectively. Then, the gradient of the potential is

$$\vec{\nabla} V(\vec{r}) = a[\hat{r} \cos(\alpha - |\phi - \phi_0|) + \hat{\phi} \sin(\alpha - |\phi - \phi_0|)] \times \delta(\vec{r} - \vec{r}_0 - \vec{a}), \quad (9)$$

where δ is the Dirac delta function and α is the angle that the vector \vec{a} , with origin at the point \vec{r}_0 and end at a point on the circumference of the potential ($|\vec{a}| = a$) makes with the vector \vec{r}_0 . In the limit $a \rightarrow 0$, we write

$$\vec{\nabla} V(\vec{r}) \approx a[\hat{r} \cos(\alpha) + \hat{\phi} \sin(\alpha)] \delta(\vec{r} - \vec{r}_0), \quad (10)$$

where $\cos(\alpha)$ and $\sin(\alpha)$ are anisotropic coupling constants. A vortex-antivortex pair solution with ‘‘center of mass’’ at

the origin is given by $\theta_{2\nu} = \arctan[(y-P)/x] - \arctan[(y+P)/x]$, where $R=2P$ is the distance between the vortex centers. The energy of a pair is $E_{2\nu} = \pi^2 J + 2\pi J \ln(R/a)$. Note that the energy $E_{2\nu}$ increases with increasing R , implying an attractive force between vortices of opposite sign. Supposing θ_1 is the deformation introduced in the vortex-antivortex structure by the absence of a spin at \vec{r}_0 we can

write $\theta = \theta_{2\nu} + \theta_1$. Rewriting $\theta_{2\nu}$ in polar coordinates and substituting $\theta = \theta_{2\nu} + \theta_1$ into Eq. (8), we obtain

$$\theta_1 = -\frac{\beta}{\pi} \ln\left(\frac{|\vec{r} - \vec{r}_0|}{a}\right), \quad (11)$$

where

$$\beta = \frac{Pa[rr_0^2 \cos(2\phi_0 - \phi) + rP^2 \cos\phi - r_0^3 \cos\phi_0 - P^2 r_0 \cos\phi_0]}{|\vec{r} - \vec{r}_0|[P^4 + r_0^4 + 2P^2 r_0^2 \cos(2\phi_0)]}. \quad (12)$$

The configuration of this deformed vortex-antivortex pair is shown in Fig. 5. As the vortex (or antivortex) center approaches the nonmagnetic impurity, the pair structure becomes more and more deformed, indicating that there is a repulsive interaction potential between each vortex core and the spin vacancy. This phenomenon is in agreement with the results of Ref. 3, where the calculations took in consideration a single vortex. In order to understand how the effective interaction potential is between the two defects, we substitute $\theta = \theta_{2\nu} + \theta_1$ into Eq. (7) to calculate the energy of the pair-impurity system E_{PI} . Unfortunately, the integral in Eq. (7) cannot be done analytically for a general impurity position, but in the special case of the spin vacancy being located at the center of mass we can solve it exactly. Using the dominant terms, the effective potential is given by

$$V_{eff} \approx \frac{a^2 J}{2\pi P^2} \left[\frac{1}{3} \ln^3\left(\frac{d}{a}\right) + \ln\left(\frac{d}{a}\right) + \frac{4\pi d}{a} \right], \quad (13)$$

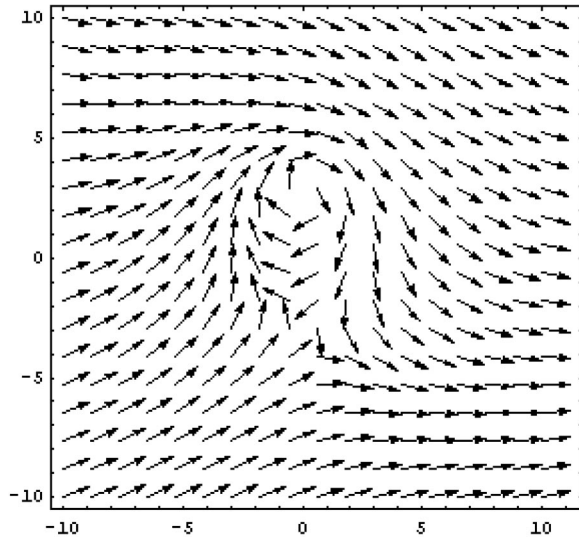


FIG. 5. A vortex pair configuration with “center of mass” located at the origin and size $R=6a$ and a spin vacancy located at (1,3). The pair configuration is deformed for large distance if vortex centers are near the impurity, increasing considerably the system energy.

where $V_{eff} = E_{PI} - E_{2\nu}$, and d is the lattice size. Since P is the distance between the vortex (or antivortex) center and the spin vacancy, this expression is very much like the effective potential obtained in Ref. 3, between a single vortex and a nonmagnetic impurity. Note that the effective interaction potential increases with decreasing $R=2P$, implying a repulsive force between vortices and impurities. In fact, the spin vacancy force obtained from Eq. (13) acts as a “repulsive force,” weakening the coupling strength between the bound vortices, and becomes stronger as P decreases. Here, the nonmagnetic impurity must repel simultaneously the two vortices in a pair, affecting the spin field for large distances (see Fig. 5). For a lattice of size d , the effective potential (13) is a minimum only if $P \rightarrow d/2$ ($R \rightarrow d$), showing the tendency of a complete separation of the vortices in a pair due to the presence of the vacancy. We conclude that static spin vacancies repel vortices, independently if they are free or bound into pairs. Based on the above results, we propose a phenomenological model to explain the behavior of the BKT temperature as a function of the impurity concentration. As discussed above, a nonmagnetic site can induce a repulsive potential between a pair vortex-antivortex in such a way that we can have the two scenarios. If the nonmagnetic impurity is in between the pair vortex-antivortex, the effective repulsive potential created tends to unbind the pair. On the other hand, if the impurity is not in between the pair, the force in the nearest vortex will be stronger than in the other and the tendency is to increase the vortex-antivortex attraction, leading to the annihilation of the pair. Then, impurities may induce either the vortex-antivortex unbinding process or pair annihilation. In a system containing a random distribution of impurities one can expect a lower density of vortices at any temperature than in a pure system due to the annihilation of pairs. Beside that, the unbinding of vortices and antivortices should occur at lower temperature, inducing the BKT transition.

Hence, we may expect a critical nonmagnetic impurity concentration in which vortex pairs are not more formed and the BKT critical temperature goes to zero. The situation is different for the case in which the nonmagnetic impurities are clustered. In this case, vortex pairs will be excited far way from the cluster in order to minimize their energies and

the cluster would have only a small influence on the vortex-antivortex unbinding. The critical temperature should not be much affected. The results presented in Fig. 4 confirm this conjecture.

V. SUMMARY

We have performed Monte Carlo simulations for the diluted planar rotator model in a square lattice. We have found that the BKT temperature decreases with increasing impurity concentration and that there is a critical impurity concentration $\rho_c \cong 0.3$ at which the transition temperature goes to zero. The interaction between a vortex pair and a static spin vacancy was studied in the continuum approximation. By considering the decoupling of vortex pairs induced by impurities we argued that the BKT critical temperature should decrease, justifying the MC simulations. Our results may also have applications for granular superconducting films such as ceramic high- T_c materials. These systems could be modeled as 2D Josephson-junction arrays because such films contain large number of Josephson boundaries between the small su-

perconducting grains forming a complex Josephson-junction network. However, the actual situation is not so ideal as the perfect array since grains with different sizes and orientations are arranged almost randomly. This makes the model with vacancies more realistic than the usual perfect array. The results can also be extrapolated to models with three spin components such as easy-plane and XY magnets. In these cases, the problem with impurities could be still more interesting since they have a true dynamics. In fact, it can shed some light on the important question of the origin of the central peak in the dynamical spin-spin correlation function in the two-dimensional anisotropic Heisenberg model.^{9–15} However, much work has to be done in order to understand those effects.

ACKNOWLEDGMENTS

This work was partially supported by CNPq and FAPEMIG (Brazilian agencies). Numerical work was done at the Laboratório de Computação e Simulação do Departamento de Física da UFJF.

¹K. Subbaraman, C.E. Zaspel, and K. Drumheller, *Phys. Rev. Lett.* **80**, 2201 (1998).

²C.E. Zaspel, K. Drumheller, and K. Subbaraman, *Phys. Status Solidi A* **189**, 1029 (2002).

³L.A.S. Mól, A.R. Pereira, and A.S.T. Pires, *Phys. Rev. B* **66**, 052415 (2002).

⁴H. Weber and P. Minnhagen, *Phys. Rev. B* **37**, 5986 (1988).

⁵P. Minnhagen, *Rev. Mod. Phys.* **59**, 1001 (1987).

⁶J.M. Kosterlitz, *J. Phys. C* **7**, 1046 (1974).

⁷L.M. Castro, A.S.T. Pires, and J.A. Plascak, *J. Magn. Magn. Mater.* **248**, 62 (2002).

⁸N. Metropolis, A.W. Rosenbluth, M.N. Rosenbluth, A.H. Teller, and E. Teller, *J. Chem. Phys.* **21**, 1087 (1953); for a review, see, e.g., *Monte Carlo Methods in Statistical Physics*, edited by K.

Binder (Springer, New York, 1979).

⁹F.G. Mertens, A.R. Bishop, G.M. Wysin, and C. Kawabata, *Phys. Rev. Lett.* **59**, 117 (1987); *Phys. Rev. B* **39**, 591 (1989).

¹⁰A.R. Pereira, A.S.T. Pires, M.E. Gouvêa, and B.V. Costa, *Z. Phys. B: Condens. Matter* **89**, 109 (1992).

¹¹A.R. Pereira and J.E.R. Costa, *J. Magn. Magn. Mater.* **162**, 219 (1996).

¹²H.G. Evertz and D.P. Landau, in *Computer Simulation Studies in Condensed Matter Physics VIII*, edited by D.P. Landau, K.K. Mon, and H.B. Schuetteler (Springer, Berlin, 1995), p. 175.

¹³J.E.R. Costa and B.V. Costa, *Phys. Rev. B* **54**, 994 (1996).

¹⁴B.V. Costa, J.E.R. Costa, and D.P. Landau, *J. Appl. Phys.* **81**, 5746 (1997).

¹⁵D.A. Dimitrov and G.M. Wysin, *Phys. Rev. B* **53**, 8539 (1996).